

Influence of three phases of El Niño-Southern Oscillation on daily precipitation regimes in China

Aifeng Lv^{1,2}, Bo Qu^{1,2}, Shaofeng Jia¹ and Wenbin Zhu¹

¹Key Laboratory of Water Cycle and Related Land Surface Processes, Institute of Geographic Sciences and Natural Resources Research, Chinese Academy of Sciences, Beijing 100101, China.

²University of Chinese Academy of Sciences, Beijing 100049, China.

*Correspondence to: Bo Qu (geo_qb@163.com) and Aifeng Lv (lvaf@163.com)

Abstract

In this study, the impacts of the El Niño-Southern Oscillation (ENSO) on daily precipitation regimes in China are examined using data from 713 meteorological stations from 1960 to 2013. We discuss the annual precipitation, frequency and intensity of rainfall events, and precipitation extremes for three phases (Eastern Pacific El Niño (EP), Central Pacific El Niño (CP), and La Niña (LN)) of ENSO events in both ENSO developing and ENSO decaying years. A Mann–Whitney U test was applied to assess the significance of precipitation anomalies due to ENSO. Results indicated that the three phases each had a different impact on daily precipitation in China and that the impacts in ENSO developing and decaying years were significantly different. EP phases caused less precipitation in developing years but more precipitation in decaying years; LN phases caused a reverse pattern. The precipitation anomalies during CP phases were significantly different than those during EP phases and a clear pattern was found in decaying years across China, with positive anomalies over northern China and negative anomalies over southern China. Further analysis revealed anomalies in frequency and intensity of rainfall accounted for these anomalies in annual precipitation; in EP developing years, negative anomalies in both frequency and intensity of rainfall events resulted in less annual precipitation while in CP decaying years, negative anomalies in either frequency or intensity typically resulted in reduced annual precipitation. ENSO events tended to trigger extreme precipitation events. In EP and CP decaying years and in LN developing years, the number of very wet days (R95p), the maximum rainfall in one day (Rx1d), and the number of consecutive wet days (CWD) all increased, suggesting an increased risk of flooding. On the other hand, more dry spells (DS) occurred in EP developing years, suggesting an increased likelihood of droughts during this phase. Possible mechanisms responsible for these rainfall anomalies are speculated by the summer monsoon and tropical cyclone anomalies in ENSO developing and decaying years.

Key words: ENSO, daily precipitation, climate extremes, summer monsoon, tropical cyclone, China

1 Introduction

The El Niño-Southern Oscillation (ENSO), a coupled ocean-atmosphere phenomenon in the tropical Pacific Ocean, exerts enormous influence on climate around the world (Zhou and Wu, 2010). Traditionally, ENSO events can be divided into a

31 warm phase (El Niño) and a cool phase (La Niña) based on sea surface temperature (SST) anomalies. An El Niño produces
32 warming SSTs in the Central and Eastern Pacific, while La Niña produces an anomalous westward shift in warm SSTs
33 (Gershunov and Barnett, 1998). Precipitation appears especially susceptible to ENSO events over a range of spatio-temporal
34 scales and therefore has been the focus of many ENSO-related studies (Lü et al., 2011). Global annual rainfall over the land
35 drops significantly during El Niño phases (Gong and Wang, 1999) and a wetter climate occurs in East Asia during El Niño
36 winters due to a weaker than normal winter monsoon (Wang et al., 2008), but these anomalies are generally reversed during La
37 Niña phases. Various studies also extensively document the teleconnections between ENSO and precipitation variation in
38 China (Huang and Wu, 1989; Lin and Yu, 1993; Gong and Wang, 1999; Zhou and Wu, 2010; Lü et al., 2011; Zhang et al., 2013;
39 Ouyang et al., 2014). Zhou and Wu (2010) found that El Niño phases induced anomalous strong southwesterly winds in
40 winter along the southeast coast of China, contributing to an increase in rainfall over southern China. In the summer after an El
41 Niño, less rainfall occurs over the Yangtze River, while excessive rainfall occurs in North China (Lin and Yu, 1993). During
42 La Niña phases, annual precipitation anomalies are spatially opposite of those during El Niño phases in China (Ouyang et al.,
43 2014). Typically, ENSO events progress over the previous winter and into the following spring/summer, thus influencing the
44 climate of China or other areas in both the developing and decaying years (Ropelewski and Halpert, 1987; Lü et al., 2011).
45 There was also a significant time lag in the responses of climate in China to ENSO evolution (Wu et al., 2004). The delayed
46 response of climate variability to ENSO provides valuable information for making regional climate predictions (Lü et al.,
47 2011).

48 ENSO events are well-known for causing extreme hydrological events (Moss et al., 1994; Chiew and McMahon, 2002;
49 Veldkamp et al., 2015) such as floods (Mosley, 2000; Räsänen and Kummu, 2013; Ward et al., 2014) and droughts (Zhang
50 et al., 2015) which in turn cause broad-ranging socio-economic and environmental impacts. Various approaches have been
51 introduced to reveal these impacts at global and regional scales. For example, Ward et al. (2014) examined peak daily
52 discharge in river basins across the world to identify flood-vulnerable areas sensitive to ENSO. Water storage is an index
53 typically used to detect frequency and magnitude of droughts during ENSO events (Veldkamp et al., 2015; Zhang et al.,
54 2015).

55 The physical mechanisms by which ENSO affects the climate of East Asia have also been discussed extensively in recent
56 decades. Many studies have revealed that anomalous summer monsoons contribute to rainfall anomalies in East Asia during
57 ENSO. A wet East Asian summer monsoon tends to occur after warm eastern or central equatorial Pacific SST anomalies
58 during the previous winter (Chang et al., 2000). Floods and droughts during ENSO are also associated with the anomalous
59 water vapor transport caused by the anomalous summer monsoon (Chang, 2004). On the other hand, tropical cyclones (TCs)
60 over the western North Pacific (WNP) are also key contributors to rainfall events in China. When TCs move westward, a huge
61 amount of moisture is transported into East Asia, accompanied by strong winds and heavy and continuous rainfall. By using

62 satellite-derived Tropical Rainfall Measuring Mission (TRMM) data, Guo et al. (2017) revealed that TCs occurring during the
63 peak TC season (from July to October, JASO) contributed ~20% of monthly rainfall and ~55% of daily extreme rainfall over
64 the East Asian coast. Strong TC activity suggests that there is excessive transport of water vapor into China.

65 Until recently, most studies have focused on changes in annual or seasonal total precipitation related to ENSO rather than
66 changes in individual precipitation events. Changes in precipitation frequency and intensity are crucial for accurate assessment
67 of ENSO impacts, but changes in mean precipitation cannot identify such changes. Recently, however, possible shifts in the
68 characteristics of precipitation events (e.g. frequency and intensity) have been highlighted in studies of global climate change
69 (Fowler and Hennessy, 1995; Karl et al., 1995; Gong and Wang, 2000). In China, it has been reported that the number of
70 wet days per year decreased in recent decades even while total annual precipitation has changed very little (Zhai et al., 2005).
71 Precipitation intensity has also changed significantly across China (Qu et al., 2016) and, as a result, drought and flood events
72 occur more frequently (Zhang and Cong, 2014). Thus, separating out the impacts of ENSO events on precipitation frequency
73 and intensity is critical to understanding ENSO-precipitation teleconnections in China. Although the link between
74 hydrological extremes and ENSO is usually discussed in the context of the physical mechanisms that influence local
75 precipitation (Zhang et al., 2015), direct precipitation indices such as the number of consecutive wet days and dry spells have
76 rarely been addressed in these studies. Thus, our knowledge of how daily precipitation extremes respond to ENSO events is
77 still very limited and requires a comprehensive set of precipitation indices that describe ENSO-induced precipitation
78 extremes. A number of recent studies suggest that a new type of El Niño should be defined that is different from the
79 canonical El Niño (Ren and Jin, 2011). This new discovered El Niño develops in regions of warming SSTs in the Pacific near
80 the International Date Line (McPhaden et al., 2006) and has been called “Dateline El Niño” or “Central Pacific (CP) El
81 Niño.” Studies have revealed that CP El Niño appears to induce climate anomalies around the globe that are distinctly
82 different than those produced by the canonical Eastern Pacific (EP) El Niño (Yeh et al., 2009). In addition, CP El Niño has
83 been occurring more frequently in recent decades (Yu and Kim, 2013). Despite a long-term focus on ENSO-climate
84 teleconnections, relatively little attention has been paid to the impacts of the new CP El Niño in China.

85 The current study aimed to provide a better understanding of how daily precipitation responds to the ENSO events over China.
86 The main objectives of this work are to document (1) any changes in daily rainfall in China during three phases of ENSO
87 events; (2) the number and duration of precipitation extremes occurring in ENSO developing and decaying years; (3)
88 anomalous summer monsoon and TC activity induced by ENSO, and their relationships with rainfall anomalies. We discuss
89 the total precipitation anomaly, anomalies of precipitation frequency and intensity patterns, and changes in precipitation
90 extremes, and propose possible mechanisms responsible for the various rainfall anomalies.

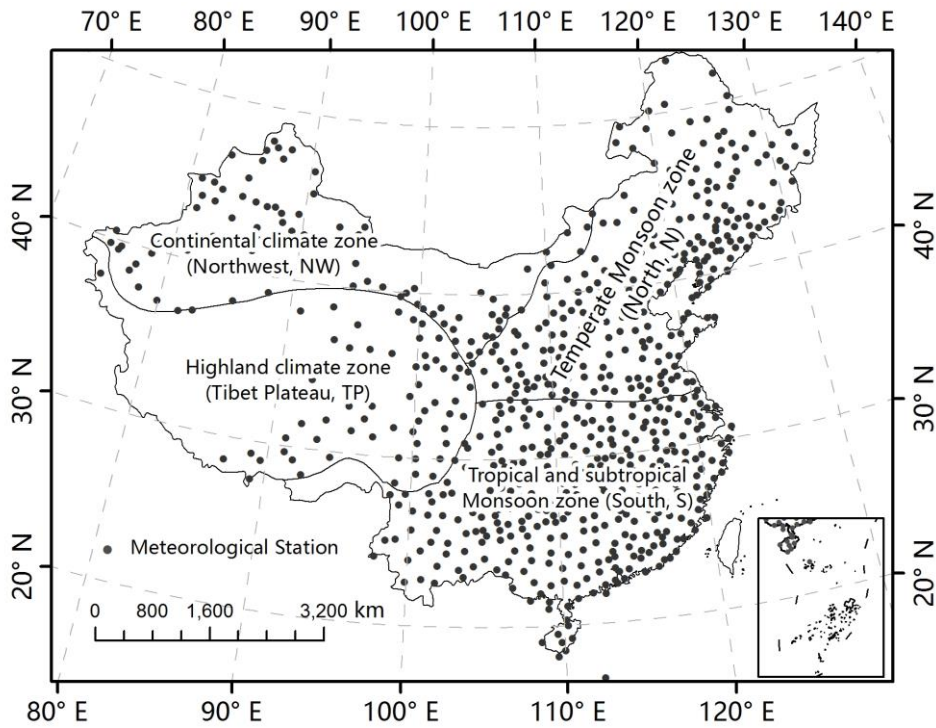
91 2 Materials and methods

92 In this study, we used daily values of climate Chinese surface stations compiled by the National Meteorological Center in
93 China. This dataset comprises detailed spatial coverage of precipitation across China, but only 400 stations were operational in
94 the 1950s (Xu et al., 2011). Non-climatic noise can complicate the accuracy of the dataset analysis (Qu et al. 2016). Stations
95 that experienced observation errors, missing values, or data homogeneity problems were omitted from analysis in this study,
96 according to similar methods used by Qian and Lin (2005). Of the 819 meteorological stations across China, data from 713
97 were ultimately selected for analysis, which covered the time period of 1960–2013 (Fig. 1). Precipitation indices were
98 calculated based on daily observations at the stations (Table 1). Annual total precipitation, as well as intensity and frequency of
99 daily precipitation events, were used to formulate precipitation characteristics. Four other indices were introduced (Zhang et al.,
100 2011), and used to analyse precipitation extremes in this study (Table 1). Precipitation indices were calculated for ENSO
101 developing and decaying years. Indices for precipitation anomalies were analysed as follows:

$$102 \quad A_{ij} = \frac{\overline{PI_{ij}} - \overline{PA_{ij}}}{\overline{PA_{ij}}}, \quad (1)$$

103 Where $\overline{PI_{ij}}$ is the average of the i precipitation index at the j meteorological station during a specific time period, and
104 $\overline{PA_{ij}}$ is the average of the i precipitation index at the j station for a multi-year average (1971–2000).

105 To quantify the variability of the summer monsoon and ENSO impacts over China, the monsoon index proposed by Wang and
106 Fan (1999) was used in this study. It is defined as the 850hPa wind speed averaged over 5 °N-15 °N, 100-130 °E minus the wind
107 speed averaged over 20 °N-30 °N, 110-140 °E, and is frequently used to study interannual and decadal variability of summer
108 monsoons over the western North Pacific-East Asian region (WNP-EA). For TC activity, the best-track dataset from the Joint
109 Typhoon Warning Center was obtained at <http://www.metoc.navy.mil/jtwc/jtwc.html>. Following the methods by Kim et al.
110 (2011), TC genesis and track density was generated for ENSO developing and decaying years for the period 1960-2013.
111 Track density anomalies are defined as annual average TC frequency during a specific type of ENSO event minus the
112 long-term mean value in each 2°×2° grid box.



113

114 **Fig. 1.** Distribution of the 713 meteorological stations used in this study. China is divided into four regions based on climatic
 115 type. The two non-monsoon regions are the continental climate zone (Northwest, NW) and the highland climate zone (Tibet
 116 Plateau, TP). The monsoon region is divided into two regions: the tropical and subtropical monsoon zone (South, S) and the
 117 temperate monsoon zone (North, N).

118

Table 1. Definitions of precipitation indices used in this study

Index	Descriptive name	Definition	Unit
P	Annual precipitation	Annual total precipitation	mm
Intensity	Daily intensity index	Average precipitation per rain event (day with precipitation > 0)	mm/day
Frequency	Number of rainy days	Annual number of rainy days	day
Rx1d	Maximum 1-day precipitation	Annual maximum 1-day precipitation	mm
R95p	Very wet day precipitation	Annual total precipitation when precipitation Greater than 95th percentile of multi-year daily precipitation*	mm
DS	dry spells	Number of consecutive dry days no less than 10	count
CWD	consecutive wet days	Number of consecutive rainy days no less than 3	count

119 *95th percentile of multi-year daily precipitation is the 95th quantile of the daily precipitation distribution over 1971–2000
 120 (Percentiles near 100 represent extremely intense precipitation).

121 In this study, two indices, created by Ren and Jin (2011) by transforming the traditionally-used Niño3 and Niño4 indices,
 122 were used to distinguish between CP and EP El Niño phases. La Niña years were identified using the methods of McPhaden
 123 and Zhang (2009). The ENSO events (1960–2013) analyzed in this study are displayed in Table 2. As an EP El Niño evolves,

124 positive SST anomalies expand latitudinally and negative signals expand eastward, reaching a maximum amplitude in
 125 autumn and winter (Feng et al., 2011). The first year was defined as the developing year of an EP El Niño in this study.
 126 Warm SST anomalies disappear and are replaced by cool anomalies in the eastern Pacific during summer of the next year
 127 (defined as the decaying year). Similarly, the emerging and vanishing years of CP El Niño and La Niña events are defined as
 128 the developing and decaying years, respectively.

129 **Table 2.** ENSO emerging years from 1960 to 2013

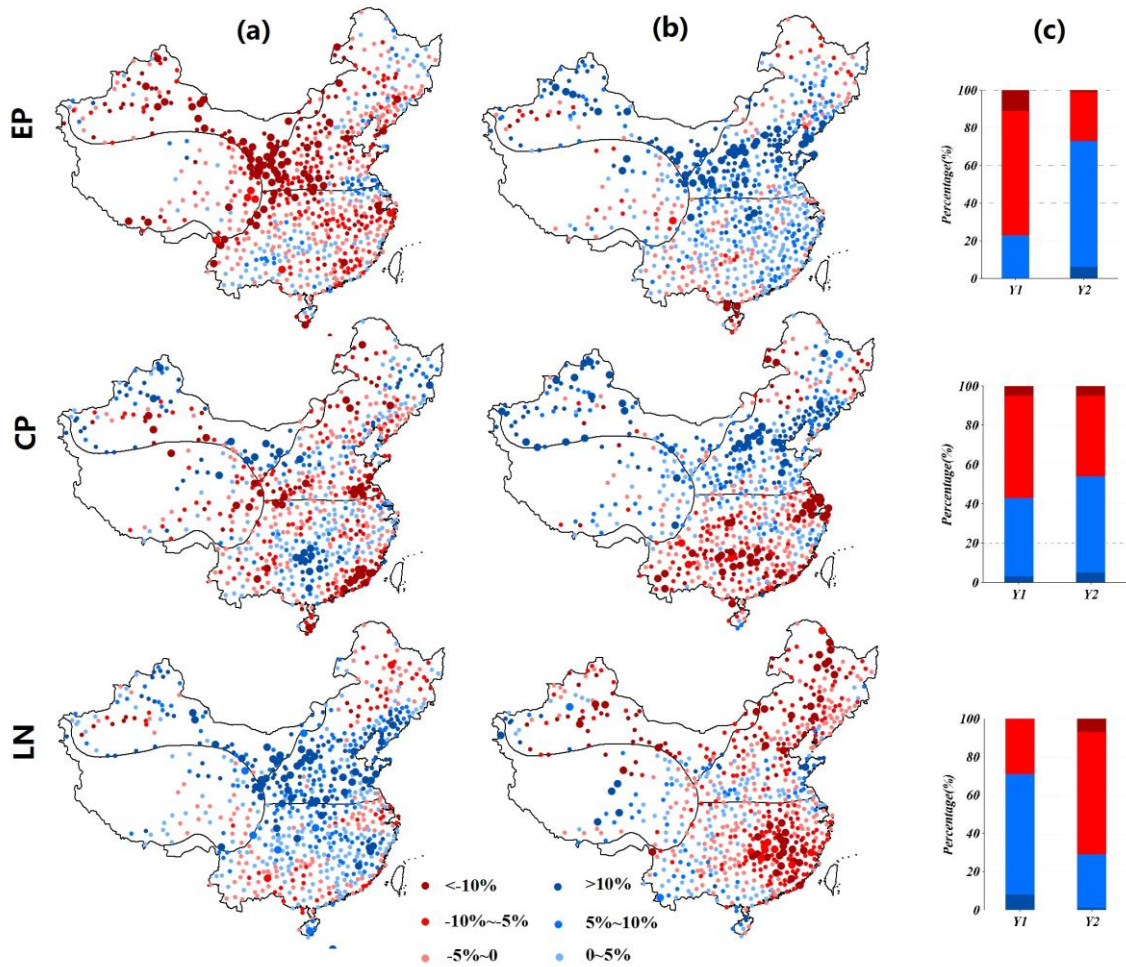
Phase	Eastern Pacific (EP)	Central Pacific (CP)	La Niña (LN)
	El Niño	El Niño	
	1963 1965 1969 1972	1968 1977 1987 1994	1964 1967 1970 1973
Year	1976 1982 1986 1991	2002 2004 2009	1975 1984 1988 1995
	1997 2006		1998 2007 2010

130 The significance of ENSO-induced precipitation anomalies is tested using a Mann–Whitney U approach. The Mann–Whitney
 131 U test is a nonparametric test applied to site data which does not conform to normality even after several transformations are
 132 performed (Teegavarapu et al., 2013). It tests whether two series are independent from each other. One series represents
 133 precipitation during an ENSO event phase (EP, CW, or LN) while the other series represents precipitation during average years.
 134 This test was applied to evaluate the significance of precipitation anomalies at a significance level of 5%.

135 **3 Results**

136 **3.1 Annual rainfall anomalies**

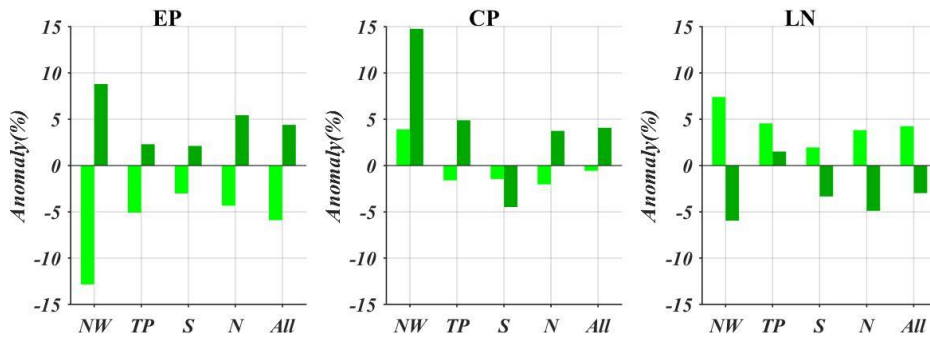
137



138

139 **Fig. 2** Anomalies of annual precipitation in developing years (a) and decaying years (b) of EP, CP, and LN phases. Stations
 140 experiencing significant anomalies are represented by large points. The percentage of stations experiencing increases or
 141 decreases in the number of rainfall anomalies are shown in (c), with significant increase (blue), increase (light blue), decrease
 142 (light red), and significant decrease (red). Y1, Y2 represent developing years and decaying years, respectively.

143 In EP developing years, 628 stations across China (~80%) had negative anomalies, and 80 of these stations the anomalies
 144 were significant. These significant stations were mainly located in the continental climate zone (NW) and the temperate
 145 monsoon zone (N) (Fig. 2). All sub-regions experienced negative average annual precipitation anomalies (Fig. 3), especially
 146 in the NW region where precipitation was 12.83% lower than the mean. Large positive anomalies of annual precipitation
 147 were found during LN developing years (Fig. 2); more than 70% of the stations showed positive anomalies, of which 10%
 148 were significant. Similarly, the stations with significant anomalies were mainly in the NW and N regions. In CP developing
 149 years, precipitation anomalies were quite different from those in EP developing years (Fig. 2). The proportion of stations
 150 with negative anomalies was 57%, but with no clear pattern of distribution.



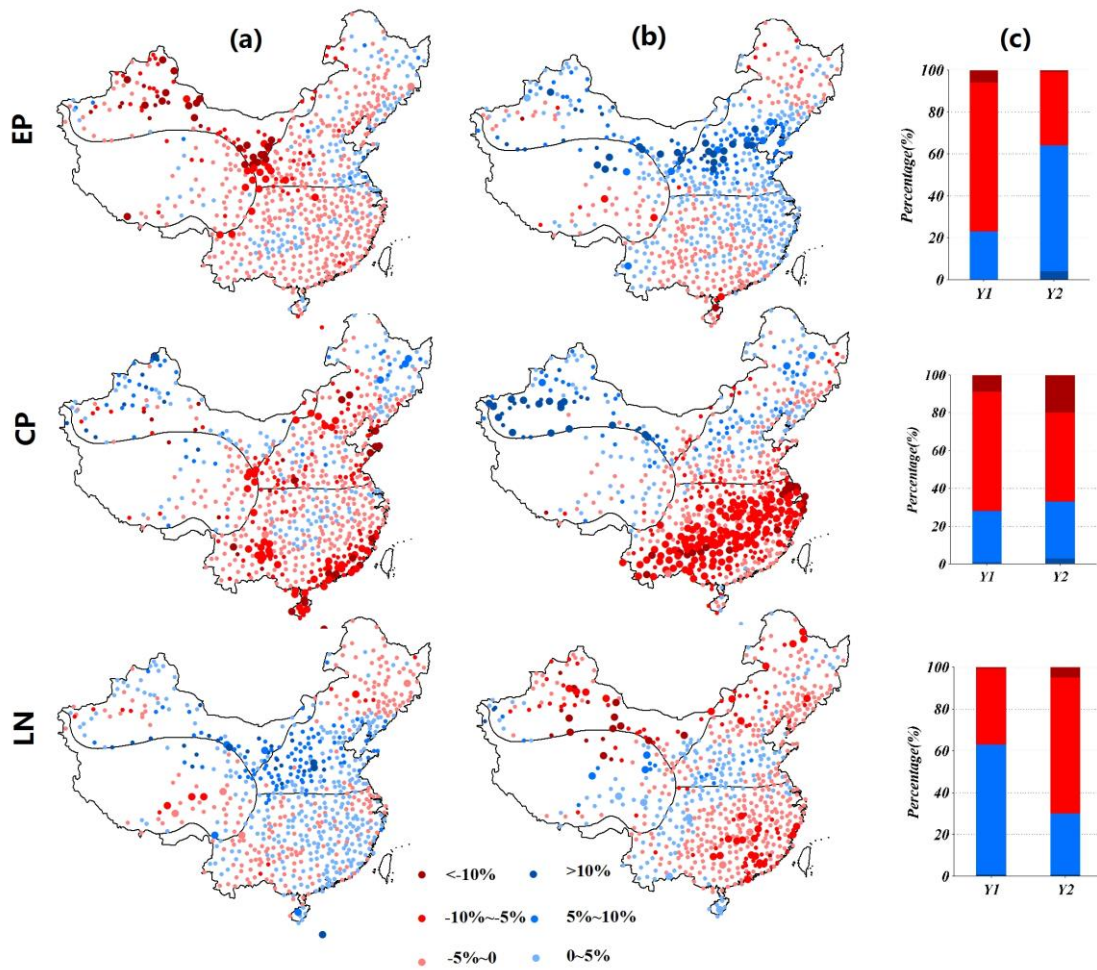
151

152 **Fig. 3** Average annual precipitation anomaly by sub-region during EP, CP, and LN phases. Light color represents developing
 153 years and dark color represents decaying years.

154 The impacts of EP phases on precipitation in decaying and developing years displayed opposite patterns. Positive anomalies
 155 were detected across China during decaying years (Fig. 2), especially in the NW and N regions at 8.8% and 8.9% higher than
 156 the mean, respectively (Fig. 3). And negative anomalies were common across China in LN decaying years (Fig. 2). In the
 157 NW region, average annual precipitation was 5.95% lower than the mean. These results suggested in both the decaying years
 158 of EP and the developing years of LN, more water vapor would be transported from the Pacific Ocean to China, while in the
 159 decaying years of LN and the developing years of EP, drier conditions would prevail. In the CP decaying phases, average
 160 annual precipitation in the NW, Tibet Plateau (TP), and N regions was much greater than the mean, but lower than the mean
 161 in the subtropical monsoon zone (S) (Fig. 3).

162 **3.2 Rainfall frequency and intensity anomalies**

163



164

165

Fig. 4 Anomalies of precipitation frequency in developing years (a) and decaying years (b) of EP, CP, and LN phases. Stations

166

experiencing significant anomalies are represented by large points. The percentage of stations experiencing anomalies of

167

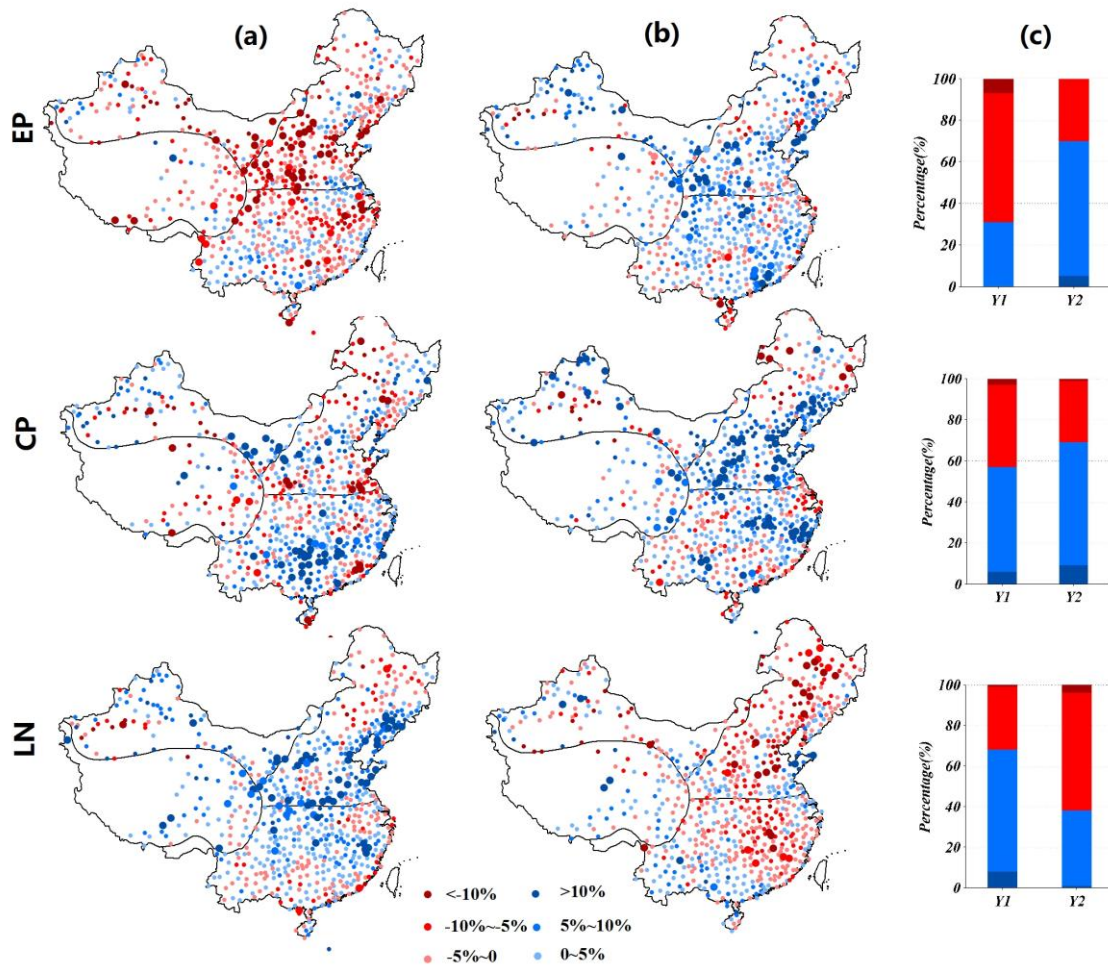
precipitation frequency are shown in (c), with significant increase (blue), increase (light blue), decrease (light red), and

168

significant decrease (red). Y1, Y2 represent developing years and decaying years, respectively.

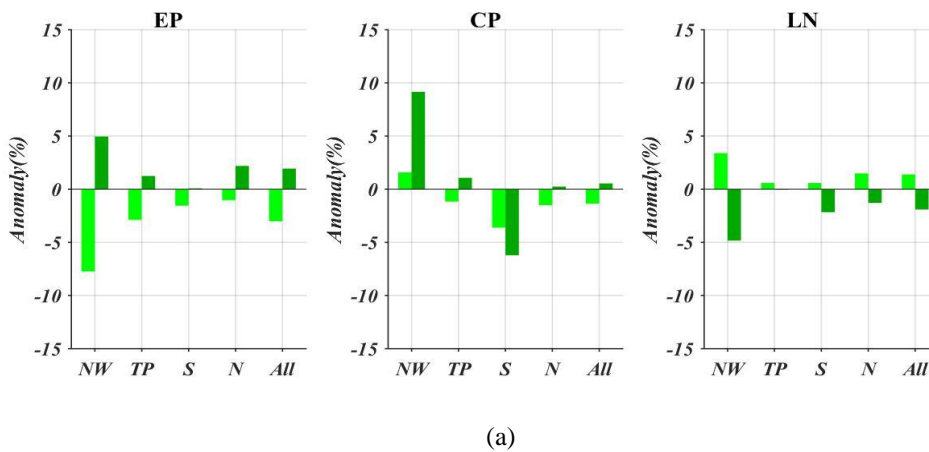
169

170



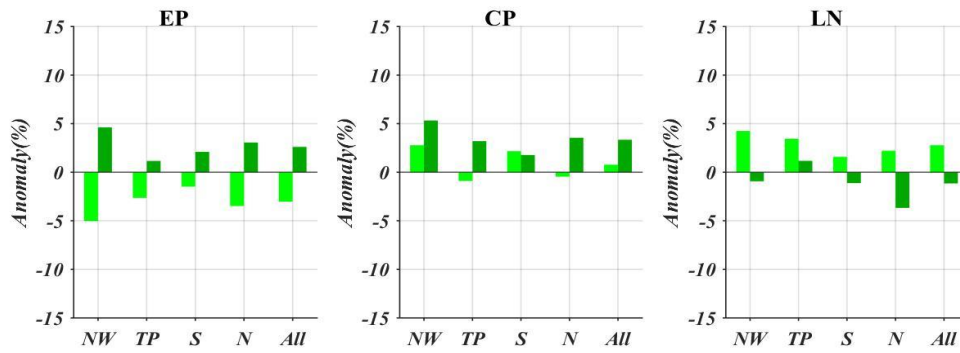
171

172 **Fig. 5** Anomalies of precipitation intensity in developing years (a) and decaying years (b) of EP, CP, and LN phases. Stations
 173 experiencing significant anomalies are represented by large points. The percentage of stations experiencing anomalies of
 174 precipitation frequency are shown in (c), with significant increase (blue), increase (light blue), decrease (light red), and
 175 significant decrease (red). Y1, Y2 represent developing years and decaying years, respectively.



176

177



(b)

Fig. 6 Average anomalies of precipitation frequency (a) and precipitation intensity (b) by sub-region during EP, CP, and LN phases. Light color represents developing years and dark color represents decaying years.

In EP developing years, only negative anomalies of precipitation intensity and frequency occurred, with decreases of 3.04% and 3.01%, respectively, across all of China (Fig. 6). Stations with significant decreases in precipitation frequency were mainly located in the NW region (Fig. 4) and stations with significant decreases in precipitation intensity were mainly located in the N region (Fig. 5). In contrast, anomalies of precipitation intensity and frequency in EP decaying years were positive, presenting a reverse pattern to the developing phase. Anomalies of precipitation intensity and frequency were also positive in LN developing years, with stations of significance concentrated in the N region.

In the CP phases, anomalies of precipitation intensity and frequency displayed more complex patterns than those in the EP years. In developing years, slightly more than half of the stations experienced positive anomalies of precipitation intensity (Fig. 5), while more than 70% experienced negative anomalies in precipitation frequency (Fig. 4). Of the stations experiencing negative precipitation frequency anomalies, 64 were significant (Fig. 4) and were concentrated in the S and N regions (Fig. 4). Precipitation frequency anomalies also formed a clear distribution pattern in CP decaying years (Fig. 4). Of all the meteorological stations, 145 (20%) experienced significant negative anomalies and were concentrated in the S region. In contrast, all regions experienced positive anomalies of precipitation intensity.

In general, anomalies of total precipitation tend to result from changes in both the frequency and intensity of precipitation events. Combined with the analysis in section 3.1, the results suggest that increases in precipitation frequency and intensity during EP decaying years and LN developing years resulted in the positive anomalies of annual precipitation across China during these phases. And the decreases in precipitation frequency and intensity during EP developing years and LN decaying years resulted in the negative anomalies of annual precipitation. But, in the CP phases, few regions displayed such clear relationships between anomalies in total precipitation and precipitation events. For example, in the N region, precipitation frequency changed very little, and the observed positive anomalies of annual rainfall in CP decaying phases appear to have resulted from increased precipitation intensity. Likewise, in the S region, precipitation intensity increased by 1.77% even though the precipitation frequency and total precipitation decreased.

204 **3.4 Precipitation extremes**

205 ENSO can trigger extreme hydro-climatological events such as floods, droughts, and cyclones (Zhang et al., 2013). Table 3
 206 shows the average percent change in the number of extreme precipitation events (anomalies of precipitation extremes) in
 207 sub-regions and the whole of China, based on data from all meteorological stations.

208 **Table 3.** Average anomalies of precipitation extremes during EP, CP, and LN phases (%).

Years	Phases	Index	NW	TP	S	N	All
Developing years	EP	Rx1d	-7.54	-2.23	-0.34	-0.32	-2.29
		R95p	-20.68	-7.02	-4.76	-5.55	-8.78
		DS	3.38	3.93	1.94	1.59	2.67
		CWD	-15.42	-6.07	-0.95	-3.70	-5.96
	CP	Rx1d	4.89	-1.00	1.02	-2.73	0.27
		R95p	5.79	-0.99	0.57	-2.93	0.28
		DS	-2.12	0.83	-0.10	2.18	0.34
		CWD	9.91	-2.11	-3.66	-3.33	-0.42
	LN	Rx1d	4.87	4.73	3.40	2.84	3.90
		R95p	10.79	8.90	4.76	8.10	7.97
		DS	-1.21	3.58	-0.25	0.26	0.71
		CWD	8.59	2.82	0.99	4.31	3.89
Decaying years	EP	Rx1d	9.52	1.30	2.43	1.94	3.43
		R95p	15.26	5.27	4.22	7.24	7.53
		DS	-3.83	1.70	0.26	1.76	0.21
		CWD	5.96	2.22	-1.48	6.72	3.18
	CP	Rx1d	7.54	4.36	2.39	0.28	3.39
		R95p	23.32	7.99	-0.33	7.13	8.64
		DS	4.08	-3.00	13.24	-1.88	3.05
		CWD	17.78	4.14	-4.78	1.11	3.71
	LN	Rx1d	-2.50	2.22	-1.00	-4.17	-1.29
		R95p	-4.73	2.14	-3.31	-9.06	-3.67
		DS	1.85	-2.48	1.35	0.87	0.30
		CWD	-7.86	-0.70	-1.81	-3.04	-3.06

209 During EP developing years and LN decaying years China experienced markedly negative anomalies in very wet daily
 210 rainfall, as expressed by the R95p index, and positive anomalies during EP decaying years and LN developing years. These
 211 impacts of the EP and LN phases on R95p were observed in nearly all sub-regions of China. An R95p positive anomaly was
 212 also observed in CP decaying years, but only in the NW, TP, and N regions. In CP developing years, the R95p identified no
 213 significant anomalies. The Rx1d index, a measure of maximum daily rainfall, revealed similar patterns to those identified by
 214 the R95p index. Positive R95p and Rx1d values during EP and CP decaying years and LN developing years indicate an
 215 increased likelihood of extreme precipitation events during these years than normal.

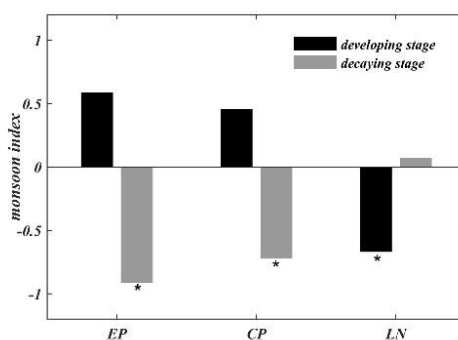
216 As shown in Table 3, negative anomalies of consecutive wet days (CWD) occurred in EP developing years and LN decaying
 217 years across China while the opposite pattern occurred in EP and CP decaying years and in LN developing years. The CWD

218 is a measure of wet conditions that is closely related to soil moisture and river runoff. A greater number of CWDs will
 219 enhance soil moisture, runoff, and the risk of floods. The NW region, a continental climate zone, is the most sensitive of
 220 China's sub-regions to ENSO events in terms of CWDs. In EP developing years, the N, TP, and NW regions experienced
 221 large decreases in CWDs (5.69%, 6.07%, and 15.42%, respectively). Such decreases have the potential to induce droughts in
 222 these sub-regions as soil moisture decreases. But the dry conditions in these sub-regions reversed in EP decaying years.
 223 Although a positive anomaly occurred in annual precipitation during CP decaying years in the N region, it experienced
 224 smaller CWD anomalies. This was possibly due to the increase in intensity of rainfall events.

225 Dry spells (DS) are extended periods of 10 days or more of no precipitation and are a strong predictor of droughts. As shown
 226 in Table 3, all sub-regions of China experienced positive anomalies in DS during EP developing years, displaying an inverse
 227 pattern to that observed for CWDs discussed above. In other words, fewer CWDs and more DS occurred simultaneously and
 228 indicated an increased risk of drought. Negative anomalies in DS were observed in the NW and N regions during EP
 229 decaying years. In CP decaying years, DS displayed dipole anomalies across China which were opposite of observed CWD
 230 patterns during the same period. But during the same years, DS anomalies were positive in the NW region even though
 231 annual precipitation had increased. DS displayed far weaker anomalies during both LN developing years and decaying years.

232 4 Discussion

233 Summer monsoons over East Asia (EA) consist of staged progressions of zonally-oriented rain belts as fronts advance and
 234 retreat. Huang and Wu's (1989) study first revealed that these summer monsoon rain belts are closely linked with ENSO
 235 cycle phases. Figure 7 shows the mean WNP-EA monsoon index and its significant difference from average conditions
 236 (1971-2000).



237
 238 **Fig. 7** The western North Pacific-East Asian (WNP-EA) summer monsoon index during different ENSO phases (average for
 239 1971-2000 is -0.007). * 95% significance

240 Results reveal that the WNP-EA monsoons tend to be weak during EP decaying years (fig. 7). Wang et al. (2001) showed
 241 that a weak WNP-EA monsoon usually features enhanced rainfall along the monsoon's front over East Asia. As for the
 242 mechanism, anomalous anticyclones in the subtropical WNP are the key systems linking the ENSO and the East Asian

243 climate (Feng et al., 2011; Wang and Chan, 2002; Wang et al., 2001; Yuan et al., 2012). An anomalous WNP anticyclone
244 during a weak WNP-EA monsoon brings plentiful moisture to southern China; meanwhile, it can also shift the ridge of the
245 sub-tropical high westward (Feng et al., 2011). When summer monsoons advance and retreat along WNP anticyclone fronts,
246 heavy and continuous rainfall typically develop along the monsoon fronts (Chang, 2004). In this study, our examination of
247 variations in precipitation anomalies reveals that rainfall is largely enhanced over the NW and N region during EP decaying
248 years (fig. 2).

249 Weak WNP-EA summer monsoons also tend to occur during CP decaying and LN developing years (fig. 7). Typically,
250 anomalous WNP anticyclones originate and develop during the previous autumn in the El Niño developing year and persist
251 until the following spring and summer before intensities decrease (Wang et al., 2003). Yuan et. al (2012) found that WNP
252 anticyclones display distinct location, intensity, and lifetime evolutions in the CP and EP El Niños due to the different
253 anomalous SSTs in the equatorial Pacific. The EP El Niño tends to create stronger, wider, and longer-lived WNP
254 anticyclones than the CP El Niño (Shi and Qian, 2018). In terms of rainfall pattern, the CP El Niño induced asymmetric
255 anomalies that do not follow the patterns seen in the EP El Niño (fig. 2). For example, during CP decaying years, the S
256 region experienced a negative annual precipitation anomaly. Anomalous WNP anti-cyclones may explain this incongruity
257 between the influences of the EP and CP El Niño phases, reflecting the potential for changes in atmospheric diabatic forcing
258 over the tropics. In contrast, weak WNP-EA summer monsoons during LN developing years possibly correlate with the
259 disappearance of EP during decaying years when WNP anticyclones tend to re-invigorate and extend northwestward and
260 inland (Feng et al., 2011). Precipitation anomalies in China also reveal a marked consistency between EP decaying years and
261 LN developing years (fig. 2).

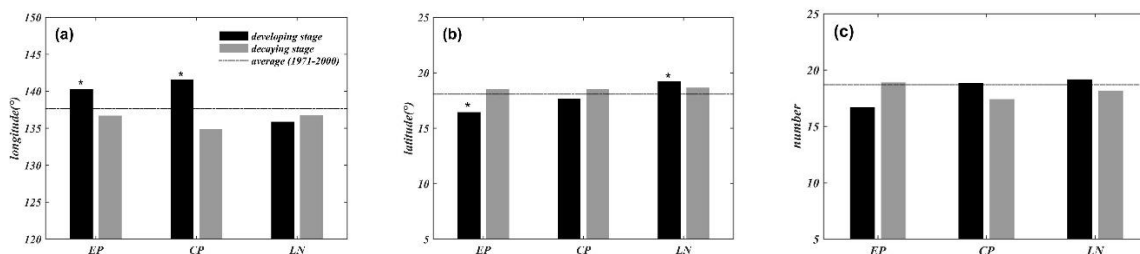
262 Fig. 7 further reveals that strong WNP-EA summer monsoons occur during EP or CP developing years, although not
263 significantly. However, only the EP developing stage induces a negative rainfall anomaly over China (fig.2). Similar results
264 were observed by Wu et. al (2003), who documented seasonal rainfall anomalies in East Asia, finding that the rainfall
265 correlation distribution displayed pronounced differences between developing and decaying ENSO years. A reverse
266 monsoon signal between developing and decaying years suggests that WNP anticyclones respond in terms of location and
267 intensity to the evolution of SST anomalies over the tropical Pacific (Chang, 2004).

268 Using a climate model, Chou et al. (2012) found that changes in precipitation frequency and intensity are closely associated
269 with changes in atmospheric water vapor and vertical motion. As demonstrated by Chou et al. (2012), an increase in water
270 vapor reduces the magnitude of the vertical motion required to generate the same strength of precipitation, resulting in an
271 increase in precipitation frequency and intensity. Therefore, large amounts of water vapor transported during EP and CP
272 decaying years, or during LN developing years, when WNP-EA summer monsoons are relatively weak may enhance both
273 precipitation frequency and intensity. On the other hand, atmospheric vertical motion also tends to be intense during these

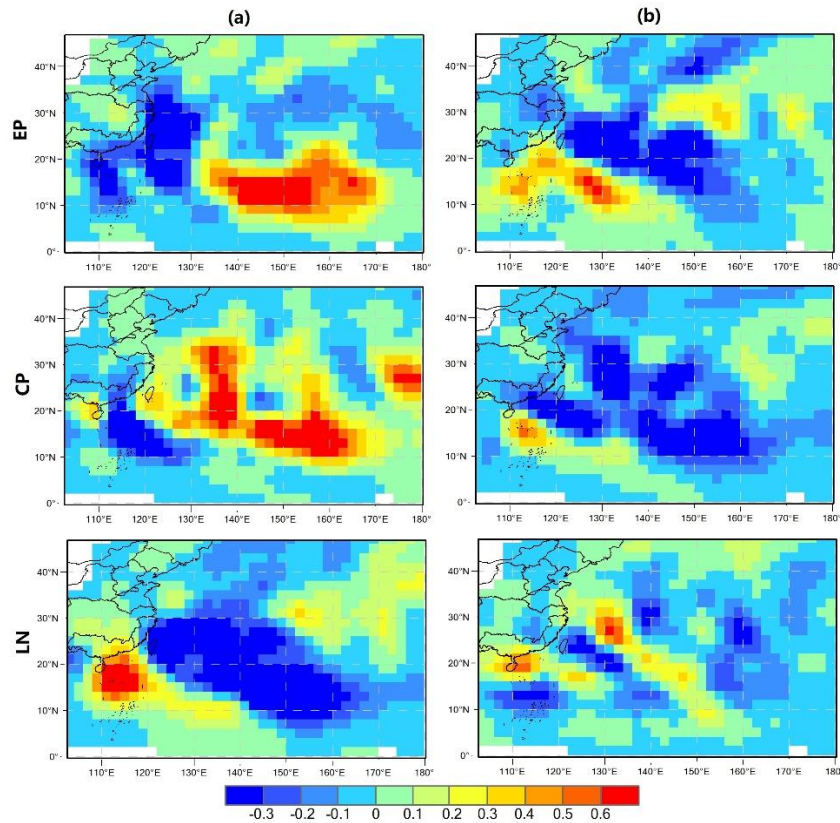
274 periods, as summer monsoons over China feature strong southerly winds (Chen et al., 2013). This leads to further anomalous
 275 R95p, Rx1d, and CWD, resulting in increased flood risk during these years (table 3). However, a reduction in water vapor
 276 availability and vertical motion may occur during EP and CP developing years as WNP-EA summer monsoons tend to be
 277 strong (fig. 7), resulting in a negative anomaly in frequency and intensity of precipitation (fig. 4 & 5).

278 In addition, the relative stability of the atmosphere tends to reduce the frequency and intensity of precipitation by reducing
 279 vertical motion (Chou et al., 2012). The WNP subtropical high is a prime circulation system over the WNP-EA and
 280 anomalies of location and intensity largely affect summer monsoon activities in East Asia (Wang et al., 2013). Huang and
 281 Wu (1989) found that when the location of a subtropical high is shifted unusually northward, hot and dry weather occurs in
 282 East China due to the dominance of the stable atmosphere. The location and intensity of subtropical highs are also closely
 283 associated with the development of WNP anticyclones, and the northward shift usually coincides with strong WNP-EA
 284 summer monsoons (Wang et al., 2001). Therefore, anomalous WNP subtropical highs possibly exacerbate negative
 285 precipitation frequency anomalies and positive DS anomalies in the S region during LN decaying years (fig4 & table 3). This
 286 may also explain the strong reductions in precipitation frequency in the S region during CP decaying years (fig.4), because
 287 WNP anticyclones display different anomalies than EP phases.

288 ENSO is one of the most important factors affecting TC activity over the WNP (Wu et. al, 2012). In this study, the
 289 modulation of TC activity by ENSO was analyzed during developing and decaying phases for the period 1960-2013. Fig. 8
 290 shows ENSO-induced anomalies in terms of TC number and location of formation. Track density anomalies are shown in fig.
 291 9.



292
 293 **Fig. 8** Anomalies in TC genesis longitude (a), latitude (b), and number (c) during JASO over the WNP. The dashed line
 294 indicates the average value for 1971-2000. * 95% significance.



295

296 **Fig. 9** Track density anomalies during JASO in developing years (a) and decaying years (b) of EP, CP, and LN phases.

297

298

299

300

301

302

303

304

305

306

307

308

309

310

311

312

Although the total number of TSs formed in the WNP did not vary significantly from year to year, TCs tended to form further east and south during EP developing years (fig. 8). This shift in the location of TC genesis constrained TCs westward propagation into East Asia (Wang and Chan, 2002). Therefore, track density was largely reduced over the coast of China (fig. 9). This suggests that the EP developing stage induces a smaller impact by TC on rainfall in China. Conversely, during LN developing years, TCs tend to form further north (fig. 8), and the track density shows a remarkable increase in the South China Sea (fig. 8). The enhancement of TC activity tends to induce heavier rainfall events, leading to positive anomalies of precipitation intensity, Rx1d, R95p, and CWD during such years (fig. 4 & 5, table 3). TCs during CP developing years also form at higher latitudes than during EP phases, but the average latitude is lower than during the LN phase (fig. 8). In contrast, the CP developing stage increases track density from the central–western Pacific to the eastern China coast and decreases it over the South China Sea (fig. 9). Kim et al. (2011) revealed that a shift in TC genesis location during CP years is closely associated with anomalous westerly winds induced by the westward shift in ocean heating, and that this shift further provides more favorable conditions for westward TC propagation. Zhang et. al (2012) also claimed that TCs during CP summers are more likely to make landfall over East Asia because of a westward shift in subtropical highs and a northward shift in TC genesis. However, TCs during CP developing years do not exert significant rainfall anomalies over China. The anomalous WNP-EA summer monsoons induced by ENSO may further explain this discrepancy. As discussed above, the strong WNP-EA monsoons during CP developing years do not induce negative rainfall anomalies over China (fig. 7). This suggests

313 that enhanced TC activity may cause a reduction in rainfall along monsoon fronts, resulting in neutral conditions over China.
314 However, further studies are needed to examine how the CP developing stage influences rainfall over China.
315 In contrast, no significant shifts in the locations of TC genesis occurred during decaying years (fig. 8). This suggests that the
316 impact of ENSO on TC formation may decrease after ENSO maturation. However, nearly opposite TC track density patterns
317 occur over the WNP during developing and decaying years of an EP or CP (fig.9). For example, in EP decaying years, TC
318 activity increased in the South China Sea and decreased from the western Pacific to the eastern China coast. This shift in
319 track density affected water vapor transport and contributed to a reversed pattern of rainfall anomalies between developing
320 and decaying years.

321 **5 Summary**

322 Using a nonparametric hypothesis test, this study investigated the impacts of three different ENSO phases on daily rainfall
323 regimes in China during the past half century. Rainfall data collected from meteorological stations across the country
324 revealed that the impacts of the three phases were significantly different from each other on a daily time scale. ENSO events
325 triggered large changes in the frequency and intensity of precipitation events and in the occurrence of precipitation extremes.
326 This finding is significant because past studies examining teleconnections between ENSO events and climate variation in
327 China have primarily focused on annual and/or monthly rainfall rather than on daily precipitation events. Since ENSO events
328 can be predicted one to two years in advance using various coupled ocean/atmosphere models (Lü et al., 2011), this study
329 can provide a means of climate prediction on a daily time scale and enable the prioritization of adaptation efforts ahead of
330 extreme events.

331 Previous studies have revealed that some regions in China are especially vulnerable to ENSO events via teleconnections,
332 such as the South China Sea (Qu et al., 2004; Rong et al., 2007; Zhou and Chan, 2007; Liu et al., 2011) and the Yangzi River
333 (Huang and Wu, 1989; Tong et al., 2006; Zhang et al., 2007; Zhang et al., 2015). However, using daily precipitation indices,
334 we found that the continental climate zone (NW) is more sensitive than other regions to ENSO events due to its high
335 incidence and magnitude of anomalous precipitation events (Fig. 4 & 5 and Table 3). For example, the NW region
336 experienced the largest R95p and CWD anomalies during all ENSO event phases. In an earlier study on daily river
337 discharges at a global scale, Ward et al. (2014) found that ENSO has a greater impact on annual floods in arid regions than in
338 non-arid regions. In China, Hui et al.(2006) analyzed interdecadal variations in summer rainfall in response to the SST
339 anomaly over the Niño-3 region. They found that summer rainfall in northwestern China was well-predicted by ENSO
340 events between 1951–1974 (Hui et al., 2006). But little research has been conducted on the mechanisms behind climatic
341 responses to ENSO events in China's continental climate zone because most studies have focused on monsoon zones
342 (Matsumoto and Takahashi, 1999; Wen et al., 2000; Wang et al., 2008; Zhou and Wu, 2010).

343 Although the primary physical processes and mechanisms responsible for precipitation anomalies have been discussed in the
344 context of summer monsoons and TC activity, approaches to understanding the forces influencing daily precipitation events
345 coinciding with ENSO are more complex than those directed toward precipitation influences on a monthly or annual scale.
346 This complexity can be illustrated by the observation that in CP decaying years, the N region experienced a positive anomaly
347 of annual precipitation due to an increase in precipitation intensity, but the S region experienced a negative anomaly due to a
348 large decrease in precipitation frequency. Therefore, even though some physical mechanisms may explain precipitation
349 variabilities related to ENSO events, there is a need for more research on the mechanisms driving atmospheric circulation to
350 advance our understanding of these influences over temporal and spatial scales. In addition, the year-to-year variability of
351 East Asian summer monsoons are likely influenced by complex air-sea-land and tropical-extratropical interactions in
352 addition to ENSO events. These interactions may include Tibetan Plateau heating, Eurasian snow cover, and polar ice
353 coverage (Wang et al., 2000). Other factors that may contribute to precipitation anomalies in China during ENSO events
354 include forces that generate large-scale circulation events, such as global warming. In a warmer climate, water vapor in the
355 atmosphere tends to increase, which destabilizes the atmosphere and enhances precipitation (Chou et al., 2012). Therefore,
356 most positive precipitation anomalies are expected from a theoretical point of view in spite of the associated atmospheric
357 circulation does not change too much.

358 **Acknowledgements.** This study was funded by the National Key Research and Development Program of China (Grant No.
359 2016YFC0401307) and the National Natural Science Foundation of China (Grant No. 41671026). We appreciate the editors and
360 anonymous reviewers for their constructive comments on improving the original manuscript.

361 **References**

- 362 Chang, C. P., Zhang, Y., and Li, T.: Interannual and interdecadal variations of the East Asian summer monsoon and tropical
363 Pacific SSTs. Part I: Roles of the subtropical ridge, *Journal of Climate*, 13, 4310-4325, 2000.
- 364 Chang, C. P.: *East Asian Monsoon*, World Scientific, 2004.
- 365 Chen, W., Feng, J., and Wu, R.: Roles of ENSO and PDO in the link of the East Asian winter monsoon to the following
366 summer monsoon, *Journal of Climate*, 26, 622-635, 2013.
- 367 Chiew, F. H. S., and McMahon, T. A.: Global ENSO-streamflow teleconnection, streamflow forecasting and interannual
368 variability, *Hydrological Sciences Journal*, 47, 505-522, 2002.
- 369 Chou, C., Chen, C. A., Tan, P. H., and Chen, K. T.: Mechanisms for global warming impacts on precipitation frequency and
370 intensity, *Journal of Climate*, 25, 3291-3306, 2012.
- 371 Feng, J., Chen, W., Tam, C. Y., and Zhou, W.: Different impacts of El Niño and El Niño Modoki on China rainfall in the
372 decaying phases, *International Journal of Climatology*, 31, 2091-2101, 2011.

373 Fowler, A., and Hennessey, K.: Potential impacts of global warming on the frequency and magnitude of heavy precipitation,
374 *Natural Hazards*, 11, 283-303, 1995.

375 Gershunov, A., and Barnett, T. P.: Interdecadal modulation of ENSO teleconnections, *Bulletin of the American*
376 *Meteorological Society*, 79, 2715-2725, 1998.

377 Gong, D. Y., and Wang, S. W.: Severe summer rainfall in China associated with enhanced global warming, *Climate Research*,
378 16, 51-59, 2000.

379 Gong, D., and Wang, S.: Impacts of ENSO on rainfall of global land and China, *Chinese Science Bulletin*, 44, 852-857, 1999.

380 Huang, R., and Wu, Y.: The influence of ENSO on the summer climate change in China and its mechanism, *Advances in*
381 *Atmospheric Sciences*, 6, 21-32, 1989.

382 Guo, L., Klingaman, N. P., Vidale, P. L., Turner, A. G., Demory, M. E., and Cobb, A.: Contribution of tropical cyclones to
383 atmospheric moisture transport and rainfall over East Asia, *Journal of Climate*, 30, 3853-3865, 2017.

384 Huang, R., and Wu, Y.: The influence of ENSO on the summer climate change in China and its mechanism, *Advances in*
385 *Atmospheric Sciences*, 6, 21-32, 1989.

386 Hui, G., Yongguang, W., and Jinhai, H.: Weakening significance of ENSO as a predictor of summer precipitation in China,
387 *Geophysical research letters*, 33, 2006.

388 Karl, T. R., Knight, R. W., and Plummer, N.: Trends in high-frequency climate variability in the twentieth century, *Nature*, 377,
389 217-220, 1995.

390 Kim, H. M., Webster, P. J., and Curry, J. A.: Modulation of North Pacific tropical cyclone activity by three phases of ENSO,
391 *Journal of Climate*, 24, 1839-1849, 2011.

392 Lü, A., Jia, S., Zhu, W., Yan, H., Duan, S., and Yao, Z.: El Niño-Southern Oscillation and water resources in the headwaters
393 region of the Yellow River: links and potential for forecasting, *Hydrology and Earth System Sciences*, 15, 1273-1281, 2011.

394 Lin, X. C., and Yu, S.Q.: El Nino and rainfall during the flood season (June-August) in China, *Acta Meteorologica Sinica*, 51,
395 434-441, 1993.

396 Liu, Q., Feng, M., and Wang, D.: ENSO-induced interannual variability in the southeastern South China Sea, *Journal of*
397 *oceanography*, 67, 127-133, 2011.

398 Matsumoto, J., and Takahashi, K.: Regional differences of daily rainfall characteristics in East Asian summer monsoon season,
399 *Geographical review of Japan, Series B.*, 72, 193-201, 1999.

400 McPhaden, M. J., Zebiak, S. E., and Glantz, M. H.: ENSO as an integrating concept in earth science, *science*, 314, 1740-1745,
401 2006.

402 McPhaden, M. J., and Zhang, X.: Asymmetry in zonal phase propagation of ENSO sea surface temperature anomalies,
403 *Geophysical Research Letters*, 36, 2009.

404 Mosley, M. P.: Regional differences in the effects of El Niño and La Niña on low flows and floods, *Hydrological Sciences*
405 *Journal*, 45, 249-267, 2000.

406 Moss, M. E., Pearson, C. P., and McKerchar, A. I.: The Southern Oscillation index as a predictor of the probability of low
407 streamflows in New Zealand, *Water Resources Research*, 30, 2717-2723, 1994.

408 Ouyang, R., Liu, W., Fu, G., Liu, C., Hu, L., and Wang, H.: Linkages between ENSO/PDO signals and precipitation,
409 streamflow in China during the last 100 years, *Hydrology and Earth System Sciences*, 18, 3651-3661, 2014.

410 Qian, W., and Lin, X.: Regional trends in recent precipitation indices in China, *Meteorology and Atmospheric Physics*, 90,
411 193-207, 2005.

412 Qu, B., Lv, A., Jia, S., and Zhu, W.: Daily Precipitation Changes over Large River Basins in China, 1960–2013, *Water*, 8,
413 10.3390/w8050185, 2016.

414 Qu, T., Kim, Y. Y., Yaremchuk, M., Tozuka, T., Ishida, A., and Yamagata, T.: Can Luzon Strait transport play a role in
415 conveying the impact of ENSO to the South China Sea? *Journal of Climate*, 17, 3644-3657, 2004.

416 Räsänen, T. A., and Kummu, M.: Spatiotemporal influences of ENSO on precipitation and flood pulse in the Mekong River
417 Basin, *Journal of Hydrology*, 476, 154-168, 2013.

418 Ren, H. L., and Jin, F. F.: Niño indices for two types of ENSO, *Geophysical Research Letters*, 38, 2011.

419 Rong, Z., Liu, Y., Zong, H., and Cheng, Y.: Interannual sea level variability in the South China Sea and its response to ENSO,
420 *Global and Planetary Change*, 55, 257-272, 2007.

421 Ropelewski, C. F., and Halpert, M. S.: Global and regional scale precipitation patterns associated with the El Niño/Southern
422 Oscillation, *Monthly weather review*, 115, 1606-1626, 1987.

423 Shi, J., and Qian, W.: Asymmetry of two types of ENSO in the transition between the East Asian winter monsoon and the
424 ensuing summer monsoon, *Climate Dynamics*, 1-20, 2018.

425 Teegavarapu, R. S. V., Goly, A., and Obeysekera, J.: Influences of Atlantic multidecadal oscillation phases on spatial and
426 temporal variability of regional precipitation extremes, *Journal of Hydrology*, 495, 74-93, 2013.

427 Tong, J., Qiang, Z., Deming, Z., and Yijin, W.: Yangtze floods and droughts (China) and teleconnections with ENSO activities
428 (1470–2003), *Quaternary International*, 144, 29-37, 2006.

429 Veldkamp, T. I., Eisner, S., Wada, Y., Aerts, J. C., and Ward, P. J.: Sensitivity of water scarcity events to ENSO-driven climate
430 variability at the global scale, *Hydrology and Earth System Sciences*, 19, 4081, 2015.

431 Wang, B., and Fan, Z.: Choice of South Asian summer monsoon indices, *Bulletin of the American Meteorological Society*, 80,
432 629-638, 1999.

433 Wang, B., Wu, R., and Fu, X.: Pacific-East Asian teleconnection: how does ENSO affect East Asian climate? *Journal of*
434 *Climate*, 13, 1517-1536, 2000.

435 Wang, B., Wu, R., and Lau, K.: Interannual variability of the Asian summer monsoon: Contrasts between the Indian and the
436 western North Pacific–East Asian monsoons, *Journal of climate*, 14, 4073-4090, 2001.

437 Wang, B., and Chan, J. C.: How strong ENSO events affect tropical storm activity over the western North Pacific, *Journal of*
438 *Climate*, 15, 1643-1658, 2002.

439 Wang, B., Clemens, S. C., and Liu, P.: Contrasting the Indian and East Asian monsoons: implications on geologic timescales,
440 *Marine Geology*, 201, 5-21, 2003.

441 Wang, B., Xiang, B., and Lee, J. Y.: Subtropical high predictability establishes a promising way for monsoon and tropical
442 storm predictions, *Proceedings of the National Academy of Sciences*, 110, 2718-2722, 2013.

443 Wang, L., Chen, W., and Huang, R.: Interdecadal modulation of PDO on the impact of ENSO on the East Asian winter
444 monsoon, *Geophysical Research Letters*, 35, 2008.

445 Ward, P. J., Eisner, S., Flörke, M., Dettinger, M. D., and Kummu, M.: Annual flood sensitivities to El Niño–Southern
446 Oscillation at the global scale, *Hydrology and Earth System Sciences*, 18, 47-66, 2014.

447 Wen, C., Graf, H. F., and Ronghui, H.: The interannual variability of East Asian winter monsoon and its relation to the summer
448 monsoon, *Advances in Atmospheric Sciences*, 17, 48-60, 2000.

449 Wu, M., Chang, W., and Leung, W.: Impacts of El Niño–Southern Oscillation events on tropical cyclone landfalling activity in
450 the western North Pacific, *Journal of Climate*, 17, 1419-1428, 2004.

451 Wu, R., Hu, Z. Z., and Kirtman, B. P.: Evolution of ENSO-related rainfall anomalies in East Asia, *Journal of Climate*, 16,
452 3742-3758, 2003.

453 Xu, X., Du, Y., Tang, J., and Wang, Y.: Variations of temperature and precipitation extremes in recent two decades over China,
454 *Atmospheric Research*, 101, 143-154, 2011.

455 Yeh, S. W., Kug, J. S., Dewitte, B., Kwon, M. H., Kirtman, B. P., and Jin, F. F.: El Niño in a changing climate, *Nature*, 461,
456 511-514, 2009.

457 Yuan, Y., Yang, S., and Zhang, Z.: Different evolutions of the Philippine Sea anticyclone between the eastern and central
458 Pacific El Niño: Possible effects of Indian Ocean SST, *Journal of Climate*, 25, 7867-7883, 2012.

459 Yu, J. Y., and Kim, S. T.: Identifying the types of major El Niño events since 1870, *International journal of climatology*, 33,
460 2105-2112, 2013.

461 Zhai, P., Zhang, X., Wan, H., and Pan, X.: Trends in total precipitation and frequency of daily precipitation extremes over
462 China, *Journal of climate*, 18, 1096-1108, 2005.

463 Zhang, Q., Xu, C. Y., Jiang, T., and Wu, Y.: Possible influence of ENSO on annual maximum streamflow of the Yangtze River,
464 China, *Journal of Hydrology*, 333, 265-274, 2007.

465 Zhang, Q., Li, J., Singh, V. P., Xu, C. Y., and Deng, J.: Influence of ENSO on precipitation in the East River basin, South China,
466 Journal of Geophysical Research: Atmospheres, 118, 2207-2219, 2013.

467 Zhang, X., Alexander, L., Hegerl, G. C., Jones, P., Tank, A. K., Peterson, T. C., . . . Zwiers, F. W. Indices for monitoring
468 changes in extremes based on daily temperature and precipitation data. Wiley Interdisciplinary Reviews: Climate Change, 2(6),
469 851-870, 2011.

470 Zhang, X., and Cong, Z.: Trends of precipitation intensity and frequency in hydrological regions of China from 1956 to 2005,
471 Global and Planetary Change, 117, 40-51, 2014.

472 Zhang, Z., Chao, B., Chen, J., and Wilson, C.: Terrestrial water storage anomalies of Yangtze River Basin droughts observed
473 by GRACE and connections with ENSO, Global and Planetary Change, 126, 35-45, 2015.

474 Zhou, L. T., and Wu, R.: Respective impacts of the East Asian winter monsoon and ENSO on winter rainfall in China, Journal
475 of Geophysical Research: Atmospheres, 115, 2010.

476 Zhou, W., and Chan, J. C.: ENSO and the South China Sea summer monsoon onset, International Journal of Climatology, 27,
477 157-167, 2007.

478 Zhang, W., Graf, H. F., Leung, Y., and Herzog, M.: Different El Niño types and tropical cyclone landfall in East Asia, Journal
479 of Climate, 25, 6510-6523, 2012.